Hue University Journal of Science: Natural Science
Vol. 130, No. 1D, 39–45, 2021

pISSN 1859-1388
eISSN 2615-9678

IMPACT OF MAXWELLIAN AVERAGED NEUTRON CAPTURE CROSS-SECTIONS FOR $^{182}W(n,\gamma)^{183}W$ REACTION ON W ISOTOPIC COMPOSITIONS

Nguyen Nhu Le*

University of Education, Hue University, 34 Le Loi St., Hue, Vietnam

* Corresponding author: Nguyen Nhu Le <nnle@hueuni.edu.vn>

(*Received: 2 June 2021; Accepted: 4 August 2021*)

Abstract. The W isotopic compositions have been investigated within the classical approach to the *s*-process nucleosynthesis. The Maxwellian averaged neutron capture cross-sections (MACS) adopted in the calculation are obtained from the TALYS-1.9 code with four nuclear level density models: the constant temperature plus Fermi gas, the back-shifted Fermi gas, the generalised superfluid, and the microscopic method of Goriely. The results show that the uncertainty from MACS values is already propagated in the W isotopic ratios, and the generalised superfluid prediction exhibits the largest deviation from the observed $^{182}W/^{184}W$ ratio. In addition, since branching points have not been considered in this work, the MACS values of the $^{182}W(n,\gamma)^{183}W$ reaction are found not to affect the estimated $^{183}W/^{184}W$ ratio.

Keywords: neutron capture reaction, *s*-process, isotopic composition

1 Introduction

In 1957, Burbidge et al. [1] and Cameron [2] independently and thoroughly described nuclear processes forming the atomic nuclei located beyond the iron peak. In these studies, heavy element compositions were assumed to be created via neutron capture reactions, particularly the rapid (*r*) and slow (*s*) processes. The *s* (*r*) neutron capture produces neutron-rich nuclei with a slow (rapid) time scale compared with the β-decay rate, and these reactions take place in an environment with a very high-neutron density such as an asymptotic giant branch (AGB) phases [3], or the stellar explosions [4]. However, several observed proton-rich isotopes could not be produced via neutron capture processes, and a proton capture (*p*) process is, instead, responsible for creating their abundances. Over the decades, these two articles [1, 2] still hold in their description of the stellar processes, and their fundamental features are extensively used today.

This paper is devoted to the *s*-process in the Ta-W region. For the *s*-process occurring in AGB stars, the $^{13}C(\alpha,n)^{16}O$ reaction is the major neutron source, which operates during the inter-pulse period with a radiative condition at temperatures of approximately 0.9×10^8 K (kT ~ 8 keV). It thus leads to an efficient *s*-process [5, 6]. A second marginal neutron source originates from the $^{22}Ne(\alpha,n)^{25}Mg$ reaction at the base of the convective zone. Despite a very short-time activation compared with that of the ^{13}C source, the second neutron burst with higher neutron density and temperatures of approximately 3.0×10^9 K (kT ~ 23 keV) also has an impact on final abundances and isotopic ratios, in particular, nuclei at branching points along the *s*-process path [6].

The tantalum isotope has two branching points with atomic numbers of 182 and 183 [7]. At

the branching point ^{182}Ta, the *s*-process flow produces ^{182}W, ^{183}W, and ^{184}W via ^{182}Ta(β,ν)^{182}W(n,γ)^{183}W(n,γ)^{184}W. Meanwhile, when the second burst of neutrons is activated, ^{182}Ta preferably captures a thermal neutron and generates ^{183}Ta. After being created by slow neutron capture of ^{183}Ta, the isotope ^{184}Ta undergoes β-decay and leads to the formation of ^{184}W. Consequently, these branch point isotopes strongly affect the tungsten isotopic ratios, which can be determined by using either stellar evolution models (see, for example, the FRUITY database [8]) or a classical analysis. The latter method consists of a formulation in terms of $\langle\sigma_i\rangle N_{si}$ products, where N_{si} is the fractional *s*-abundance of nucleus *i*, and $\langle\sigma_i\rangle$ is its Maxwellian averaged neutron capture cross-sections (MACS) [9]. MACS within the classical formula are evaluated at the neutron energy equal to 30 KeV and can be used to determine stellar reaction rates. This approach was found to be a useful tool for calculating the *s*-process abundances in the solar system [5] despite its simple and straightforward description.

Ávila et al. reported the W isotopic compositions measured in stardust SiC grains from the Murchison meteorite, and the results were compared with *s*-process synthesis calculations [7]. The comparisons show anomalous W isotopic ratios lower than those observed from the solar system. These discrepancies reflect that nuclear inputs and nucleosynthesis calculations should continue to be improved to provide a reliable description of the abundance distribution. The impact of nuclear parameters on the final abundances studied in Ref. [10] has shown that uncertainties from neutron capture rates of heavy isotopes produce an average error in a range from 10 to 25%. Notably, the percentage significantly increases for nuclei at the branching points [11]. Recommended MACS values of nuclei relevant to the *s*-process nucleosynthesis can be found in the compilation by Bao et al. [12], or the Karlsruhe Astrophysical Database of Nucleosynthesis in Stars (KADoNiS), version 0.3 [13]. However, the latter database provides an uncertainty of 25% for their recommended MACS values, determined by averaging recent evaluations (see, for example, TENDL-2015 [14]). Hence, regardless of the current full MACS data, the effect of calculated MACS values within microscopic nuclear reaction models on W isotopic ratios presented here is particularly important for understanding neutron capture astrophysics.

The Hauser-Feshbach (HF) formulation [15] has been extensively used for evaluating MACS values in the *s*-process nucleosynthesis calculation, wherein the nuclear level density (NLD), the radiative strength function (RSF), and the neutron optical model potential (*n*-OMP) are essential nuclear input parameters. Although the last decades have seen enormous progress in experimental studies of the NLD [16, 17], the available data is not adequate for modelling stellar evolution because of a vast reaction network consisting of about a thousand isotopes participating in the *s*-process [18]. Because of this, the former input has been theoretically estimated with phenomenological methods [19-21] and microscopic approaches [22-24].

In the present paper, we study the impact of calculated MACS values of ^{182}W(n,γ)^{183}W within different NLD models on W isotopic compositions. The selected NLD theories used in the calculation consist of the constant temperature plus Fermi gas (FG) [19], the back-shifted Fermi gas (BSFG) [20], the generalised superfluid (SF) [21], and the microscopic nuclear level densities based on Skyrme force models (Goriely-Skyrme) [22]. The four NLD models are used as inputs to the TALYS-1.9 code [14] to obtain the radiative neutron capture cross-sections of ^{182}W(n,γ)^{183}W

pISSN 1859-1388
eISSN 2615-9678

and corresponding MACS predictions. The latter results are employed to calculate W isotopic compositions by using the classical stellar model of the *s*-process. Our paper is organized as follows: The theoretical aspects of MACS and the classical approach to the *s*-process calculation are briefly reviewed in Section 2. In Section 3, we plotted the numerical results of neutron capture cross-sections and MACS values within different models of NLD and compared with those taken from the literature [12, 25]. In addition, the comparisons of the evaluated W isotopic ratios of ^{182}W/^{184}W and ^{183}W/^{184}W with the observed solar ratios [26] are also presented. Finally, the conclusions are outlined in Section 4.

2 Maxwellian-averaged cross-sections and the classical *s*-process model

The average cross-sections for a Maxwellian spectrum are read as $\sigma_{MACS}(kT) = \frac{\langle \sigma v \rangle}{v_T}$ [27], where *k*, *T*, and v_T are the Boltzmann constant, the temperature of the system, and the relative velocity of a target and neutrons, respectively. The mean thermal velocity v_T has the form $v_T = \sqrt{2kT/\mu}$, where the reduced mass of the target-neutron system, μ, equals $m_1 m_2/(m_2 + m_1)$, and m_1 and m_2 are the masses of the neutron and the target. The Maxwellian-averaged cross-sections are then given by [28]

$$\sigma_{MACS}(kT) = \frac{2}{\sqrt{\pi}}(kT)^{-2}\int_0^{\infty}\sigma(\mathrm{E})E\exp\left(-\frac{E}{kT}\right)dE, \quad (1)$$

where *E* is the energy in the center-of-mass frame.

The classical *s*-process model was first described in detail by Clayton et al. [29]. They reported that the *s*-process abundances found in nature could be computed by adopting an exponential distribution of neutron exposures ϱ(τ), $\rho(\tau) = \frac{G_{main}\cdot N_{\odot}^{56}}{\tau_0}\exp\left(-\frac{\tau}{\tau_0}\right)$, with τ being the time-integrated neutron flux. The fraction G_{main} of the observed iron abundance $N_{\odot}^{56}$, which is required as seed, has the value of $G_{\mathrm{main}} = 0.057$ [9], and the mean neutron exposure, $\tau_0 = 0.295$ mb^{-1}. In such a case, one can obtain an analytical solution if the neutron capture rates' possible time dependence $\lambda_n = N_n\langle\sigma\rangle v_T$ is ignored, where N_n is the neutron density. Specifically, the temperature and neutron density N_n are assumed constant throughout the *s*-process. The product of the stellar cross-section and the *s*-abundance can then be expressed as [9]

$$\langle\sigma\rangle_{(A)}N_{s(A)} = \frac{G_{main}\cdot N_{\odot}^{56}}{\tau_0}\prod_{i=56}^{A}\left(1+\frac{1}{\tau_0\langle\sigma\rangle_i}\right)^{-1}. \quad (2)$$

In the *s*-process nucleo-synthesis calculation, we select the appropriate nuclei located in the *s*-path from ^{56}Fe to ^{184}W. It is found that the neutron capture flow is in equilibrium among the magic neutron numbers, and the $\langle\sigma\rangle_{(A)}N_{s(A)}$ curve is almost unchanged. Furthermore, as stated in Ref. [9], 0.04% of the ^{56}Fe abundance in nature is considered as a seed, and each seed nucleus captures about 15 neutrons. This finding implies that the main *s*-process component is produced in low-mass thermally pulsing AGB stars [6]. Over decades, the classical approach has well described this main component for isotopes of masses numbers in the range of 88–208 [5].

3 Numerical calculations and discussions

In this section, we numerically calculate W isotopic compositions from the NLD data derived from the FG, BSFG, SF, and Goriely-Skyrme methods. Firstly, the obtained NLD parameters of the four models were used to compute the ^{182}W(n,γ)^{183}W capture cross-sections. As shown in Fig. 1, the agreement between the cross-section estimated with the Goriely-Skyrme approach and the experiments is satisfactory in the neutron energy range less than 0.1 MeV. In addition, in

this region, the two predictions of the FG and BSFG methods produce almost the same results, which also slightly derivate from the experimental curve; whereas, large discrepancies are observed for the calculation based on the SF model. In the higher energy region, the estimated neutron capture cross-sections adopting the four NLD models are similar, and both methods under-predict the data. It turns out that the influence of NLD models on thermal-neutron capture cross-sections is less pronounced at neutron energies between 0.1 and 1 MeV. The resulting cross-sections are then used to calculate MACS values through Eq. (4).

A comparison of the MACS values at the *s*-process energy of 30 keV, obtained by employing the four NLD theories, with the data extracted from the compilation by Bao et al. [12] is shown in Fig. 2a. The MACS values predicted via the FG, BSFG, SF, and Goriely-Skyrme methods are 273.8, 283.2, 306.2, and 264.2 mb, respectively. A remarkable agreement with the recommended MACS value of 274 mb is found in the estimation of the FG model. Additionally, the BSFG and Goriely-Skyrme results also describe the experiments well, with an error of less than 4%, while the deviation from the data of SF results is the largest, with an error being approximately 12%. These findings are reasonably obtained since the MACS values in Eq. (1) are proportional to the neutron capture cross-section, as we can collate Fig. 1 with Fig. 2a.

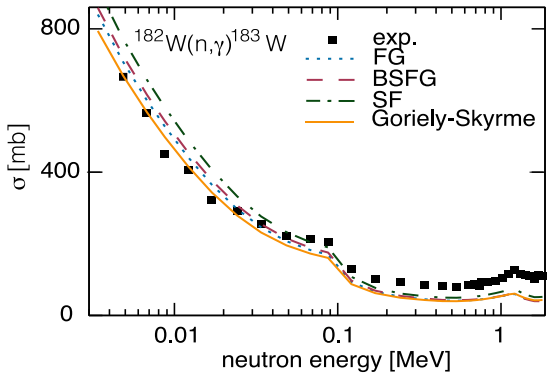

Fig. 1. (Color online) ^{182}W(n,γ)^{183}W capture cross-sections as functions of thermal neutron energy. Calculated results within the FG (dotted line), BSFG (dashed line), SF (dot-dash line), and Goriely-Skyrme (solid line) models of NLD are compared with those taken from the experiments [25]

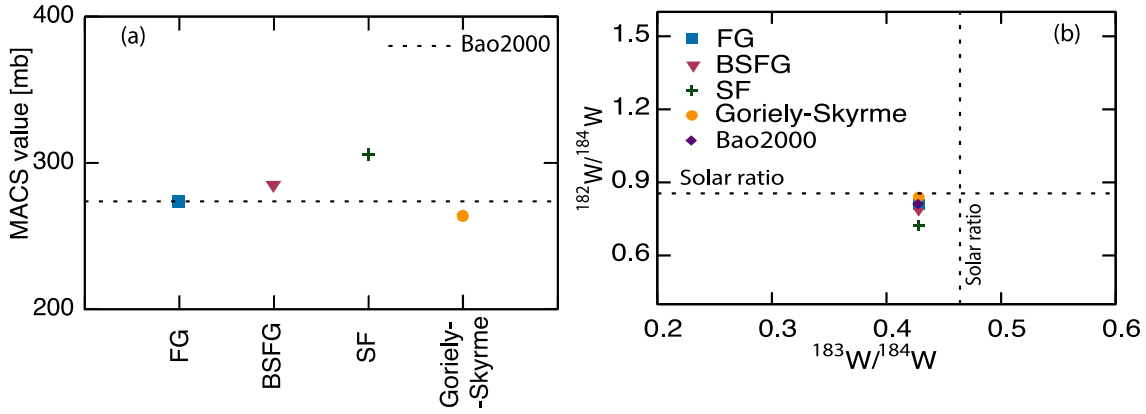

Fig. 2. (Color online) (a) MACS values at 30 keV for the ^{182}W(n,γ)^{183}W reaction are calculated by applying different NLD models. Experimental data (dotted line) taken from Ref. [12]; (b) The ^{182}W/^{184}W ratio plotted against the ^{183}W/^{184}W ratio for different MACS values in Fig. 2a. Experimental data extracted from [26]

pISSN 1859-1388
eISSN 2615-9678

The theoretical MACS estimations and the data recommended by Bao are now used as inputs to the *s*-process nucleosynthesis formula given in Eq. (2), and the obtained W isotopic compositions are illustrated in Fig. 2b. The number of the seed nuclei $N_{\odot}^{56}$ and the solar W isotopic ratios are extracted from Ref. [26]; whereas, the MACS values for nuclei along the *s*-path from ^{56}Fe to ^{182}Ta are collected from Bao's data. As expected, the uncertainty of the MACS values is already propagated in the W isotopic ratios. Notably, there is a significant difference between the ^{182}W/^{184}W ratio computed with the SF theory and those measured (Fig. 2b), and the others fit the data well. Furthermore, the ^{183}W/^{184}W ratio is unaffected by the MACS values calculated in this work, and it is lower than the solar ratio because the branching points at ^{182}Ta and ^{183}Ta have not been considered so far. As the second neutron source of ^{22}Ne operates with a higher neutron density, these branching points are activated, resulting in a small change of the Ta isotopic abundances. However, to obtain the final W isotopic abundances with the treatment of branching, one has to determine the initial abundances left from the previous ^{13}C "pocket" phase, which is only calculated in stellar evolution models.

4 Conclusions

We have used NLD calculations within the FG, BSFG, SF, and Goriely-Skyrme approaches as inputs to the TALYS code, and the obtained results are the cross-sections of radiative neutron capture reactions on the ^{182}W nucleus, corresponding to MACS predictions and W isotopic compositions. Among the four NLD models, the microscopic Goriely-Skyrme shows a good agreement with the neutron capture cross-section data. At neutron energies in the region from 0.1 to 1 MeV, both theoretical estimations are lower than those of the data, and the impact of different NLDs on the cross-sections is insignificant. Next, the computed MACS values for the ^{182}W(n,γ)^{183}W reaction show that the FG, BSFG, and Goriely-Skyrme models fit the data taken from the compilation by Bao et al. At the same time, the most significant discrepancy is observed for the SF model. The W isotopic compositions are evaluated by using different MACS estimations and data. Within the classical *s*-process model framework, the W isotopic ratios are evaluated by using different MACS estimations and data. It is found that the MACS values of the ^{182}W(n,γ)^{183}W reaction primarily affect the final ^{182}W/^{184}W ratio, and the most significant deviation from the natural ratio is in the case of SF input. Besides, no deviations in the ^{183}W/^{184}W ratio are visible since branching has not been considered. Hence, the final ^{182}W/^{184}W ratio is strongly influenced by the MACS values and the NLD models. The classical *s*-process is found to provide a good description of the *s*-only isotopes. For calculating the final abundances with branching problems, stellar evolution models should be used, where the neutron densities and temperatures in the inter-shells of stars and thus branching ratios are known.

Funding statement

This research is supported by the National Foundation for Science and Technology Development of Vietnam (NAFOSTED) under grant number 10/2020/STS02.

References

1. Burbidge E, Burbidge G, Fowler W, Hoyle F. Synthesis of the Elements in Stars. Reviews of Modern Physics. 1957;29:547-655.
2. Cameron AGW. Stellar evolution, nuclear astrophysics, and nucleogenesis. Second edition. Canada; 1957.
3. Cristallo S, Straniero O, Gallino R, Piersanti L, Dominguez I, Lederer MT. Evolution, nucleosynthesis, and yields of low-mass asymptotic giant branch stars at different metallicities. The Astrophysical Journal. 2009;696:797-820.

4. Wehmeyer B, Pignatari M, Thielemann FK. Galactic evolution of rapid neutron capture process abundances: the inhomogeneous approach. Monthly Notices of the Royal Astronomical Society. 2015;452:1970-1981.
5. Kappeler F, Gallino R, Bisterzo S, Aoki W. The s-process: Nuclear physics, stellar models, and observations. Reviews of Modern Physics. 2011;83:157-193.
6. Bisterzo S, Gallino R, Kappeler F, Wiescher M, Imbriani G, Straniero O, et al. The Branchings of the Main s-process: Their Sensitivity to α-induced Reactions on 13C and 22Ne and to the Uncertainties of the Nuclear Network. Monthly Notices of the Royal Astronomical Society. 2015;449:506-527.
7. Ávila JN, Lugaro M, Ireland TR, Gyngard F, Zinner E, Cristallo S, et al. Tungsten isotopic compositions in stardust SiC grains from the Murchison meteorite: Constraints on the s-process in the Hf-Ta-W-re-Os region. The Astrophysical Journal. 2012;744:49-92.
8. Cristallo S, Straniero O, Piersanti L, Gobrecht D. Evolution, nucleosynthesis, and yields of AGB stars at different metallicities. III. Intermediate-mass models, revised low-mass models, and the pH-FRUITY interface. The Astrophysical Journal Supplement Series. 2015;219:40-61.
9. Kappeler K, Gallino R, Busso M, Picchio G, Raiteri CM. S-Process nucleosynthesis: Classical approach and asymptotic giant branch models for low-mass stars. The Astrophysical Journal. 1990;354:630-643.
10. Vinyoles N, Serenelli A. A sensitivity study of s-process: the impact of uncertainties from nuclear reaction rates. Journal of Physics: Conference Series. 2016;665:012028-4.
11. Cescutti G, Hirschi R, Nishimura N, Hartogh JWd, Rauscher T, Murphy ASJ, et al. Uncertainties in s-process nucleosynthesis in low-mass stars determined from Monte Carlo variations. Monthly Notices of the Royal Astronomical Society. 2018;478(3):4101-4127.
12. Bao Z, Beer H, Kappeler F, Voss F, Wisshak K, Rauscher T. Neutron cross sections for nucleosynthesis studies. Atomic Data and Nuclear Data Tables. 2000;76:70-154. DOI: https://doi.org/10.1006/adnd.2000.0838
13. Data extracted using the KADoNiS On-Line Data Service. URL: https://www.kadonis.org
14. Koning AJ, Rochman D. Modern Nuclear Data Evaluation with the TALYS Code System. Nuclear Data Sheets 2012;113:2841-2934.
15. Hauser W, Feshbach H. The Inelastic Scattering of Neutrons. Physical Review. 1952;87:366-373.
16. Utsunomiya H, Renstrom T, Tveten GM, Goriely S, Ari-izumi T, Filipescu D, et al. γ-ray strength function for thallium isotopes relevant to the 205Pb-205Tl chronometry. Physical Review C. 2019;99:024609-8.
17. Netterdon L, Endres A, Goriely S, Mayer J, Scholz P, Spieker M, et al. Experimental constraints on the γ-ray strength function in 90Zr using partial cross sections of the 89Y(p,γ)90Zr reaction. Physical Letter B. 2015;744:358-362.
18. Nishimura N, Hirschi R, Rauscher T, Murphy AStJ, Cescutti G. Uncertainties in s-process nucleosynthesis in massive stars determined by Monte Carlo variations. Monthly Notices of the Royal Astronomical Society. 2017;469:1752-1767.
19. Gilbert A, Cameron AGW. A composite nuclear-level density formula with shell corrections. The Canadian Journal of Physics. 1965;43:1446-1496.
20. Vonach H, Uhl M, Strohmaier B, Smith BW, Bilpuch EG, Mitchell GE. Comparison of average s-wave resonance spacings from proton and neutron resonances. Physical Review C. 1988;38:2541-2549.
21. Ignatyuk AV, Weil JL, Raman S, Kahane S. Density of discrete levels in 116Sn. Physical Review C. 1993;47:1504-1513.
22. Goriely S, Tondeur F, Pearson JM. A Hartree-Fock nuclear mass table. Atomic Data and Nuclear Data Tables. 2001;77:311-381.
23. Goriely S, Hilaire S, Koning AJ. Improved microscopic nuclear level densities within the HFB plus combinatorial method. Physical Review C. 2008;78:064307-14.
24. Phuc LT, Hung NQ, Dang ND, Huong LTQ, Anh NN, Duy NN, et al. Role of exact treatment of thermal pairing in radiative strength functions of 161-163Dy nuclei. Physical Review C. 2020;102:061302(R)-6.
25. Macklin RL, Drake DM, Arthur ED. Neutron Capture Cross Sections of 182W, 183W, 184W, and 186W from 2.6 to 2000 keV. Nuclear Science and Engineering. 1983;84:98-119.
26. Lodders K, Palme H, Gail HP. Abundances of the elements in the solar system. In Landolt-Bronstein,

pISSN 1859-1388
eISSN 2615-9678

New Series, Vol. VI/4B, Chap. 4.4, J.E. Trmper (ed.), Berlin, Heidelberg, New York: Springer-Verlag. 2009;560-630.

27. Pritychenko B, Mughabghab SF, Sonzogni AA. Calculations of Maxwellian-averaged cross sections and astrophysical reaction rates using the ENDF/B-VII.0, JEFF-3.1, JENDL-3.3, and ENDF/B-VI.8 evaluated nuclear reaction data libraries. Atomic Data and Nuclear Data Tables. 2010;96:645-748.
28. Nakagawa T, Chiba S, Hayakawa T, Kajino T. Maxwellian-averaged neutron-induced reaction cross sections and astrophysical reaction rates for kT = 1 keV to 1 MeV calculated from microscopic neutron cross section library JENDL-3.3. Atomic Data and Nuclear Data Tables. 2005;91:77-186.
29. Clayton DD, Ward RA. S-Process Studies: Exact Evaluation of an Exponential Distribution of Exposures. The Astrophysical Journal. 1974;193:397-399.